HHS Public Access

Author manuscript

Radiat Res. Author manuscript; available in PMC 2021 February 03.

Published in final edited form as:

Radiat Res. 2020 December 01; 194(6): 636–645. doi:10.1667/RADE-20-00067.1.

Ultra-High-Dose-Rate FLASH Irradiation Limits Reactive Gliosis in the Brain

Pierre Montay-Gruel[a], **Mineh Markarian**[a], **Barrett D. Allen**[a], **Jabra D. Baddour**[a], **Erich Giedzinski**[a], **Patrik Goncalves Jorge**[b], **Benoît Petit**[b], **Claude Bailat**[b], **Marie-Catherine Vozenin**[b], **Charles Limoli**[a], **Munjal M. Acharya**[a,1]

[a]Department of Radiation Oncology, University of California, Irvine, Irvine, California 92697-2695; [b]Laboratory of Radiation Oncology, Department of Radiation Oncology. Lausanne University Hospital and University of Lausanne, Lausanne, Switzerland

Abstract

Encephalic radiation therapy delivered at a conventional dose rate (CONV, 0.1–2.0 Gy/min) elicits a variety of temporally distinct damage signatures that invariably involve persistent indications of neuroinflammation. Past work has shown an involvement of both the innate and adaptive immune systems in modulating the central nervous system (CNS) radiation injury response, where elevations in astrogliosis, microgliosis and cytokine signaling define a complex pattern of normal tissue toxicities that never completely resolve. These side effects constitute a major limitation in the management of CNS malignancies in both adult and pediatric patients. The advent of a novel ultra-high dose-rate irradiation modality termed FLASH radiotherapy (FLASH-RT, instantaneous dose rates ≥ 10^6 Gy/s; 10 Gy delivered in 1–10 pulses of 1.8 μs) has been reported to minimize a range of normal tissue toxicities typically concurrent with CONV exposures, an effect that has been coined the "*FLASH effect*." Since the FLASH effect has now been found to significantly limit persistent inflammatory signatures in the brain, we sought to further elucidate whether changes in astrogliosis might account for the differential dose-rate response of the irradiated brain. Here we report that markers selected for activated astrogliosis and immune signaling in the brain (glial fibrillary acidic protein, GFAP; toll-like receptor 4, TLR4) are expressed at reduced levels after FLASH irradiation compared to CONV-irradiated animals. Interestingly, while FLASH-RT did not induce astrogliosis and TLR4, the expression level of complement C1q and C3 were found to be elevated in both FLASH and CONV irradiation modalities compared to the control. Although functional outcomes in the CNS remain to be cross-validated in response to the specific changes in protein expression reported, the data provide compelling evidence that distinguishes the dose-rate response of normal tissue injury in the irradiated brain.

INTRODUCTION

Brain exposure to ionizing radiation induces a variety of toxicities including neuroinflammation, gliosis and neurocognitive deficiencies. These toxicities are of major

[1]Address for correspondence: Department of Radiation Oncology, University of California Irvine, Medical Sciences I, Room B-149, Irvine CA 92697-2695; macharya@uci.edu.

concern in the context of radiotherapy, a frontline treatment used for the control of brain malignancies. Despite recent technological advances in treatment precision, radiation-induced side effects in the brain remain an important dose-limiting factor, affecting the tumor cure and the quality of life of cancer survivors. Recently reported studies have emphasized the benefits of ultra-high-dose-rate FLASH radiation therapy (FLASH-RT) when examining normal tissue toxicities (1, 2). Preclinical and clinical studies by us and others showed the absence of severe toxicities in several FLASH-irradiated normal tissues (3–6), along with a maintained anti-tumor effect (7). This observation has been coined as the FLASH effect. In the brain, FLASH-RT has been shown to prevent the development of short- and long-term debilitating side effects that are usually observed after conventional dose-rate (CONV) irradiation, including a preservation of cell division, neuronal structure, an absence of gliosis (microglial and astrocytic activation) along with a preservation of the long-term neurocognition associated with a reduced oxidative stress (3–5, 8). Nevertheless, biological mechanisms are still unclear and further studies are needed to fully decipher the FLASH effect.

Preclinical studies reported by us and others have found that CONV cranial irradiation induces an acute and persistent oxidative stress. This modification in homeostasis has been described as associated to molecular and cellular modifications, including an elevated chronic neuroinflammation, linked to persistent microglial activation (9–14). This pro-inflammatory status has a large negative effect on the cellular environment of the brain. Moreover, the astrocyte network represents approximately 50% of the total glial cell population and has diverse functions, including synaptic transmission modulation and secretion of growth factors (15, 16). Published studies have provided evidence that astrocytes play a role in neuropathological conditions, including neurodegeneration and neuroinflammation (17, 18). In the context of a brain injury, morphological changes are observed along with an increase in proliferation and expression of glial fibrillary acidic protein (GFAP). These long-lasting and irreversible modifications known as reactive astrogliosis have been described acutely and long-term after brain exposure to ionizing radiation (9, 19). Our data and that reported in the literature have also shown that increases in tumor necrosis factor-α (TNFα) and reduced synaptic adenosine accompanied by astrogliosis occur after brain irradiation and are associated with cognitive dysfunction (20–23).

Among the different molecular cascades responsible for the maintenance of chronic neuroinflammation, an imbalance in the complement cascade has been identified in many degenerative conditions and brain injuries, as responsible for an excessive pro-inflammatory response (24–27). Over 40 proteins in the complement system mediate immune system responses and play major roles during central nervous system (CNS) development and its protection from infections (24, 25). The expression of complement component 1q (C1q) has been found elevated in several neurodegenerative conditions in both humans and rodents (26) and has been associated with loss of synapses, neuronal complexity and cognitive dysfunction (28–30). Neuronal injury or radiation-induced activation of the complement cascade can potentially lead to pro-inflammatory microglial activation (25, 31). Activation of the complement cascade results in the production of anaphylatoxins (complement C5a and C3a) that recruit and activate microglia and astrocytes via the interaction of these

molecules with cell surface receptors (32, 33). Interestingly, the detrimental role of C3a has been described in the irradiated mouse brain associated with elevated microglial numbers and astrogliosis (34). Previous published studies from our laboratory have established the damaging role of radiation-induced chronic, elevated astrogliosis and microglial activation (35, 36).

In this work we studied the occurrence of complement activation associated with reactive astrogliosis in the FLASH-irradiated mouse brain. Using quantitative immunofluorescence, we show that, contrary to CONV irradiation, FLASH-RT does not induce reactive astrogliosis in the hippocampus of irradiated mice. Levels of GFAP, microglial C1q and toll-like receptor (TLR4) were reduced after FLASH compared to CONV irradiation, while both modalities elevated total expression of complement proteins C1q and C3 over that of nonirradiated controls. Findings here suggest that while radiation at either dose rate can trigger the complement cascade, downstream signaling leading to functional astrogliosis is not the same, pointing to a differential if not muted response of pro-inflammatory factors in the FLASH-irradiated brain.

MATERIALS AND METHODS

Animal Experiments

All animal experiments were approved by the Swiss (Vaud state approval: VD3241) and University of California, Irvine (Institutional Animal Care and Use Committee) ethics committees for animal experimentation and performed within institutional and national (Swiss and U.S. federal) guidelines. Three-to-four-month-old female wild-type mice (C57BL/6J) were maintained in standard housing conditions (20°C ± 1°C; 70% ± 10% humidity; 12:12 h light-dark schedule) and had free access to standard rodent chow and water.

Irradiation Devices

Irradiation was performed using a prototype 6-MeV electron beam linear accelerator (LINAC) of type Oriatron (eRT6; PMBAlcen), available at Lausanne University Hospital (Lausanne, Switzerland) and described elsewhere (37). Physical dosimetry has been extensively described and published to ensure reproducible and reliable biological studies (5, 37–39). This LINAC is able to produce a pulsed electron beam at a mean dose rate ranging from 0.1 Gy $\cdot$ s^{-1} (i.e., comparable to conventional dose rates used in radiation therapy) up to 5.6×10^6 Gy $\cdot$ s^{-1}, corresponding to a dose, in each electron pulse, ranging from 0.01 up to 10 Gy. In the current study 10 Gy FLASH irradiation was delivered in a single pulse of 1.8 μs. The beam parameters used throughout this study are included in Table 1. The irradiation settings corresponding to the prescription dose for mouse irradiations were determined by surface dose measurements on a 30×30 cm^2-solid water slab positioned behind a 1.7-cm-diameter aperture of a graphite applicator ($13.0 \times 13.0 \times 2.5$ cm^3), as described elsewhere (6, *58*).

Brain Irradiations

All irradiations were performed under isoflurane anesthesia. For whole brain irradiations (WBRT), the mouse head was positioned behind and in contact with the aperture of the 1.7-cm-diameter graphite applicator to irradiate the whole encephalon region, while limiting the dose to the eyes, mouth and rest of the body. Mice received a single 10 Gy dose (See Table 1 for irradiation parameters). FLASH and CONV irradiation modalities were compared.

Immunohistochemistry, Confocal Microscopy and Volumetric Quantification

At one month postirradiation, paraformaldehyde-fixed brains were isolated as described elsewhere (36). Brains were cryoprotected using a sucrose gradient (10–30%) and sectioned coronally into 30-μm-thick sections using a cryostat (Microm, Thermo Scientific™, Rockford, IL). For each end point, 3–4 representative coronal brain sections from each of 4–6 animals per experimental group were selected at approximately 15 section intervals to encompass the rostro-caudal axis from the middle of hippocampus (−2.0 to 2.9 mm from bregma) and stored in PBS. Free-floating sections were first rinsed in phosphate buffered saline (PBS), antigen retrieval was facilitated by incubation in citrate buffer (10 m*M*, pH 6.0 with 0.01% Triton™ X-100, 70°C) for 1 h followed by blocking with 10% normal donkey serum (NDS) with 0.01% Triton X-100 for 30 min. Sections were then incubated overnight in primary antibodies: rabbit anti-IBA-1 (1:500; Wako Chemicals USA, Inc., Richmond, VA), mouse or rabbit anti-GFAP (1:500), rabbit monoclonal (clone 4.8) anti-C1q (1:100; Abcam®, Cambridge, MA) or mouse anti-C3 (1:500, C3d chain; Quidel® Corp., San Diego, CA) prepared in 3% NDS in PBS with 0.01% TTX. The next day, the sections were treated with goat anti-rabbit or mouse Alexa Fluor® 488 or 568 (1:500; Invitrogen™, Carlsbad, CA) made in PBS, 0.01% TTX and 3% NDS. The sections were nuclear counterstained with DAPI (1 μmol/l in PBS, 15 min and mounted with gold slow fade antifade mounting medium (Life Technologies, Grand Island, NY).

3D Algorithm-Based Volumetric Quantification

Single- or dual-immunofluorescent-stained and mounted sections (~25 μm thick) were scanned using a laser-scanning confocal microscope (Eclipse Ti C2; Nikon, Tokyo, Japan) equipped with a 60× oil-immersion objective lens (1.4 NA) and NIS element AR module (version 4.3; Nikon). The high-resolution (1,024p) z stacks (0.5 μm step size) were scanned through the section. An adaptive, 3D blinded deconvolution method (AutoQuant X3 version 3.2; Media Cybernetics Inc., Rockville, MD) was used to deconvolute images to improve the signal resolution with respective fluorescent wavelengths (510 nm, green; 594 nm, red). The deconvoluted images were converted to IMS format for 3D algorithm-based Imaris analysis (version 9.5; Bitplane Inc., Zürich, Switzerland). In Imaris, IBA1 and GFAP were 3D modeled using the surface-rendering tool, and a 3D spot analysis was conducted for the complement component proteins (C1q, C3) or TLR4. Using an unbiased, dedicated co-localization channel, the number of complement puncta or TLR4 on the surface of glia (IBA1 or GFAP) was individually calculated by selecting spots at a distance of −0.5 μm to 0.5 μm from the surface created. The total (overall) expression and the expression level of the immunofluorescent puncta on each surface, the area and volume of IBA1 or GFAP, and the total number of puncta were used for quantitative comparison between the control and

irradiated groups. For analysis of astrogliosis, three to four individual astrocytes per brain were evaluated for the measurement of cell body and stelae volume using the surface analysis tool. To minimize batch-to-batch variations in the wet-lab experimentation (experimenter to experimenter, laser scanning confocal microscopy, etc.), we included corresponding 0 Gy control tissues for each batch of staining to compare differences with the irradiated (CONV, FLASH) groups. The data were expressed as mean volume of the immunofluorescence and number of puncta (complement proteins, TLR4) co-labeled with the glial (GFAP, IBA1) surface.

Statistical Analysis

Statistical analyses were performed using GraphPad Prism version 6 (LaJolla, CA). Given the small group size (n = 5 to 6 mince per group), we conducted a non-parametric Kruskal-Wallis H test. Once we found significant group effects, individual pairs of groups (control, CONV-RT and FLASH-RT) were compared using Mann-Whitney's non-parametric test. For all analyses $P \leq 0.05$ was considered statistically significant.

RESULTS

FLASH-RT did not Induce Astrogliosis in the Irradiated Brain

Astrocytic hypertrophy or astrogliosis is one of the consequences of radiation-induced brain injury. Our previously published study has shown a lack of microglial activation in the FLASH-irradiated compared to CONV-irradiated brains (3). To further investigate the effect of FLASH-RT on reactive gliosis, GFAP expression and astrocyte morphology were quantified in the hippocampus after CONV or FLASH irradiation. Volumetric measurement of astrocytic morphology, facilitated by 3D algorithm-based analysis of $GFAP^+$ reconstruction of the fluorescent surface, showed a significant elevation in the astrocytic hypertrophy after 10 Gy CONV irradiation that was not observed after FLASH irradiation (Fig. 1A and B). One month after CONV irradiation, hippocampal astrocytes were characterized by thicker and longer processes with elevated GFAP expression (Fig. 1B), indicating reactive astrogliosis. Interestingly, for the same dose and at the same postirradiation timepoint, no astrogliosis pattern was observed in the FLASH-irradiated hippocampus, and morphologic characteristics were comparable to controls (Fig. 1C). These assessments of astrocytic morphology indicate that FLASH-RT, as opposed to CONV-RT, does not induce hypertrophic morphology, as shown by the increased volume of soma and processes (Fig. 1A, CONV).

Expression of Complement Cascade Proteins after FLASH Irradiation was not Associated with Astrocytic Expression of TLR4

As the complement system is a potent mediator of gliosis and also has a range of non-immune functions in the CNS, including synaptic pruning, clearance of apoptotic cells and cellular debris (24, 25), we sought to determine if CONV-RT and FLASH-RT lead to differential effects on glial expression of complement cascade proteins *in vivo*. In the CNS, microglia are the prominent source of C1q, shown to play a detrimental role in a number of degenerative conditions (25). While volumetric quantification of the total C1q expression after dual immunofluorescence staining showed C1q expression elevated significantly

throughout the brain ($P = 0.02$ and 0.05; Fig. 2A and B), FLASH irradiation elevated C1q more than CONV irradiation ($P = 0.05$, Fig. 2C). Conversely, 3D volumetric analysis of the microglial ($IBA1^+$) surface co-localized with C1q showed elevated co-labeling after CONV irradiation ($P = 0.01$) but not after FLASH irradiation (Fig. 2D).

In the brain, astrocytes have been shown to express C1q under a number of pathophysiological conditions including multiple sclerosis (40), temporal lobe epilepsy (41) and Alzheimer's disease (42, 43). Thus, we quantified astrocytic immunoreactivity of C1q in the CONV- and FLASH-irradiated brain (Fig. 3A and B). GFAP-C1q co-labeling followed a similar pattern of immunoreactivity when compared to total C1q, (Fig. 2C) showing a significant increase after CONV and FLASH irradiation ($P = 0.01$, Fig. 3C). $C1q^+$ puncta were co-localized with astrocytic cell body and stelae in the brain exposed to both radiation modalities.

The downstream enzymatic cascade of complement activation generates pro-inflammatory anaphylatoxins (C3a and C5a) from the complement component C3 that mediates inflammation (32, 33). In the CNS, astrocytes are responsible for the majority of C3 production (44). Thus, the expression of C3 was analyzed one month after CONV or FLASH irradiation (Fig. 4). A significant elevation in total C3 immunoreactivity (Fig. 4A–C) was identified in both irradiation groups ($P = 0.002$, Fig. 4C). Moreover, volumetric analysis of C3 co-labeling on the $GFAP^+$ cells showed a significant increase in astrocytic C3 (Fig. 4D) after CONV and FLASH irradiation. The increase in C3 expression observed after FLASH irradiation in the absence of astrogliosis suggest a divergence in the downstream activation of the complement cascade between the irradiation modalities.

Anaphylatoxins generated by the pathologic activation of complement cascade lead to inflammation by their interaction with cell-surface receptors, including TLR4 (32, 33). To further analyze the effect of FLASH-RT on this pro-inflammatory response, astrocytic TLR4 expression was quantified one month postirradiation (Fig. 5A and B). The overall expression of TLR4 was increased significantly in the brain after CONV irradiation ($P = 0.03$, Fig. 5C). Moreover, dual immunofluorescence analysis of TLR4 and GFAP after CONV irradiation showed a significant increase of TLR4 expression at the surface of reactive astrocytes (Fig. 5B and D). In contrast, FLASH-RT did not induce any elevation of TLR4 expression at the surface of $GFAP^+$ astrocytes (Fig. 5D). These results suggest that despite an upstream activation of the complement cascade in astrocytes, FLASH-RT does not induce the expression of endogenous damage-associated molecular pattern (DAMP) receptors at the astrocyte surface in the irradiated brain, consistent with an absence of reactive astrogliosis (Fig. 1).

DISCUSSION

Our findings point to the differential involvement of inflammatory pathways in the brain in response to FLASH vs. CONV treatments. While we show that irradiation at either dose rate induces the activation of the complement cascade, reactive gliosis does not fully develop after FLASH-RT. Significant past data has implicated waves of neuroinflammation for driving persistent radiation-induced normal tissue toxicity in the brain (9, 45). This in part

provides some of the rationale for expectations that changes in inflammation might differ in the FLASH- vs. CONV-irradiated brain. While the mechanisms behind the neuroprotective effects of FLASH-RT remain partially understood, current studies have sought to uncover whether changes in the key mediators of complement cascade proteins and astrogliosis might provide a partial explanation.

Recently published studies have pointed to the importance of activated microglia in triggering reactive astrogliosis (via secretion of Il-1α, TNFα and C1qa) that perpetuate damage signatures in the CNS after insult with lipopolysaccharide (LPS) (17). Given the capability of CONV-RT modalities to persistently elevate levels of activated microglia in the brain, we reasoned that certain overlap in the LPS- vs. radiation-induced inflammatory cascade might be found by analyzing similar markers of astrogliosis. Data indicated a differential involvement of the complement cascade, where elevated astrogliosis found after CONV-RT was synchronized with elevated C3 and TLR4 expression. Expression of C1q was found to be a glia-specific response as CONV-RT elevated microglial (IBA1) C1q but not astrocytic C1q labeling. Astrocytes have been shown to express C1q in other neurodegenerative conditions including Alzheimer's disease, multiple sclerosis and temporal lobe epilepsy (41–43). Interestingly, microglial C1q was not elevated after FLASH-RT, nor was there a difference in the overall increase of astrocytic C3 immunoreactivity found between CONV and FLASH irradiation, pointing to certain similarities in the radioresponse of the complement system. Persistent inflammatory signatures resulting from cranial irradiation may also involve the downstream complement activation proteins, including C3a, iC3b and C5a, leading to the prolonged activation of microglia and astrogliosis (25, 44). Cell-type specific changes were also evident, as increased expression of TLR4 in $GFAP^+$ astrocytes after CONV-RT but not FLASH-RT points to a possible suppression of DAMP signaling in the FLASH-irradiated brain. As DAMP receptors, TLRs play important roles in elevating innate immune response against foreign pathogens that synchronizes with complement cascade activation (46, 47). Complement cascade effector proteins (C1q and iC3b) are associated with synaptic sculpting (24, 25), and may mediate previous findings showing a loss of synaptic density after CONV-RT but not FLASH-RT (3). Astrocyte intermediate filament system marker (GFAP) was used to evaluate astrogliosis and co-localization of complement proteins. Typical star-like morphology of astrocytes, revealed by GFAP immunofluorescence, underrepresent the actual volume of astrocytic processes and associated morphology (48). Therefore, GFAP co-labeling data are only partially representative of the full extent of actual morphologic co-labeling between complement and TLR4 proteins in the irradiated brain. Whether or not FLASH-RT promotes protective and/or dynamic synaptic re-modeling remains to be confirmed experimentally using complement protein or receptor knockout mice.

Importantly, our current results are consistent with our previous work, which showed FLASH-RT as opposed to CONV-RT, ameliorated radiation-induced increases in astrogliosis and microgliosis over early (2–6 weeks) to delayed (6 months) postirradiation times in both male and female mice. Despite these prior findings and our current focus on female mice, further work quantifying the response of the complement system to FLASH-RT and CONV-RT on the male brain needs to be evaluated. The need for further sex-specific studies is underscored in a recently published study by O'Banion *et al.*, showing the protective, sex-

specific effects of global complement receptor CR3 knockdown against exposure to CONV-RT radiation-mediated spine loss (49). Previously we found that FLASH-RT afforded equal neuroprotection (cognition and dendritic spines) in both male and female brains, suggesting further differences between each irradiation modality (3).

The capability of FLASH-RT to spare normal tissue toxicity without compromising tumor control stands as the hallmark of the FLASH effect. While several reviews and perspectives have been published to account for these experimental observations, one in particular has highlighted how differences in redox biology and labile iron management between tumor and normal tissue might provide some insight into the improved therapeutic index associated with FLASH-RT. The idea revolves around the hypothesis that normal tissue detoxifies hydroxyperoxides more efficiently than tumor cells, and has considerably less labile iron for catalyzing Fenton-based hydroxyl radical production (50). This then offers the assertion that the half-life of damaging radiation-induced reactive species is longer in tumor tissue saturated with FLASH-induced free radicals, an effect simply not observed in CONV-irradiated tissue due to significantly lower free radical stress. Current data highlight the complexities of different astrocytic markers, morphologies and complement activation that follow radiation exposure of the brain, and suggest that a deeper understanding of these pathways may identify some of the neuroprotective mechanisms of FLASH-RT. Nonetheless, data do show the brain to exhibit radioresponsive changes dependent upon the disparate dose rates used, and importantly for the first time, we report the actual induction of complement cascade proteins (C1q, C3) by FLASH-RT rather than the lack of activation, inhibition or suppression of pathways normally triggered by CONV-RT.

ACKNOWLEDGMENTS

This work was support by the UCI School of Medicine Faculty Pilot Research Award (no. 19900), the University of California Cancer Research Coordinating Committee award (no. CRR-19-585293) and the Health and Environmental Sciences Institute (HESI-Thrive award) to MMA. Additional support was provided by a grant from the ISREC Foundation. Additional support was provided by Biltema and Synergia (grant no. FNS CRS II5_186369), both to MCV), the National Institute of Neurological Disorders and Stroke, National Institutes of Health (NIH) [NINDS grant no. NS089575 (CLL)] and the National Cancer Institute, NIH [NCI grant no. P01CA244091 (C.L.L. and M.C.V)]. PMG was supported by a Ecole Normale Supérieure de Cachan fellowship (MESR), FNS no. 31003A_156892 and the ISREC Foundation. We also thank the Animal Facilities for the animal husbandry.

REFERENCES

1. Vozenin MC, Hendry JH, Limoli CL. Biological benefits of ultra-high dose rate FLASH radiotherapy: Sleeping Beauty awoken. Clin Oncol (R Coll Radiol) 2019; 31:407–15. [PubMed: 31010708]
2. Harrington KJ. Ultrahigh dose-rate radiotherapy: Next steps for FLASH-RT. Clin Cancer Res 2019; 25:3–5. [PubMed: 30093447]
3. Montay-Gruel P, Acharya MM, Petersson K, Alikhani L, Yakkala C, Allen BD, et al. Long-term neurocognitive benefits of FLASH radiotherapy driven by reduced reactive oxygen species. Proc Natl Acad Sci U S A 2019; 116:10943–51. [PubMed: 31097580]
4. Montay-Gruel P, Bouchet A, Jaccard M, Patin D, Serduc R, Aim W, et al. X-rays can trigger the FLASH effect: Ultra-high dose-rate synchrotron light source prevents normal brain injury after whole brain irradiation in mice. Radiother Oncol 2018; 129:582–8. [PubMed: 30177374]

5. Montay-Gruel P, Petersson K, Jaccard M, Boivin G, Germond JF, Petit B, et al. Irradiation in a flash: Unique sparing of memory in mice after whole brain irradiation with dose rates above 100 Gy/s. Radiother Oncol 2017; 124:365–9. [PubMed: 28545957]
6. Favaudon V, Caplier L, Monceau V, Pouzoulet F, Sayarath M, Fouillade C, et al. Ultrahigh dose-rate FLASH irradiation increases the differential response between normal and tumor tissue in mice. Sci Transl Med 2014; 6:245ra93.
7. Vozenin MC, De Fornel P, Petersson K, Favaudon V, Jaccard M, Germond JF, et al. The advantage of FLASH radiotherapy confirmed in mini-pig and cat-cancer patients. Clin Cancer Res 2019; 25:35–42. [PubMed: 29875213]
8. Simmons DA, Lartey FM, Schuler E, Rafat M, King G, Kim A, et al. Reduced cognitive deficits after FLASH irradiation of whole mouse brain are associated with less hippocampal dendritic spine loss and neuroinflammation. Radiother Oncol 2019; 139:4–10. [PubMed: 31253467]
9. Chiang CS, Hong JH, Stalder A, Sun JR, Withers HR, McBride WH. Delayed molecular responses to brain irradiation. Int J Radiat Biol 1997; 72:45–53. [PubMed: 9246193]
10. Limoli CL, Giedzinski E, Rola R, Otsuka S, Palmer TD, Fike JR. Radiation response of neural precursor cells: linking cellular sensitivity to cell cycle checkpoints, apoptosis and oxidative stress. Radiat Res 2004; 161:17–27. [PubMed: 14680400]
11. Lan ML, Acharya MM, Tran KK, Bahari-Kashani J, Patel NH, Strnadel J, et al. Characterizing the radioresponse of pluripotent and multipotent human stem cells. PLoS One 2012; 7:e50048. [PubMed: 23272054]
12. Acharya MM, Lan ML, Kan VH, Patel NH, Giedzinski E, Tseng BP, et al. Consequences of ionizing radiation-induced damage in human neural stem cells. Free Radic Biol Med 2010; 49:1846–55. [PubMed: 20826207]
13. Mizumatsu S, Monje M, Morhardt D, Rola R, Palmer T, Fike J. Extreme sensitivity of adult neurogenesis to low doses of X-irradiation. Cancer Res 2003; 63:4021–7. [PubMed: 12874001]
14. Parihar VK, Acharya MM, Roa DE, Bosch O, Christie LA, Limoli CL. Defining functional changes in the brain caused by targeted stereotaxic radiosurgery. Translational Cancer Research 2014; 3:124–37. [PubMed: 24904783]
15. Bushong EA, Martone ME, Jones YZ, Ellisman MH. Protoplasmic astrocytes in CA1 stratum radiatum occupy separate anatomical domains. J Neurosci 2002; 22:183–92. [PubMed: 11756501]
16. Araque A, Carmignoto G, Haydon PG, Oliet SH, Robitaille R, Volterra A. Gliotransmitters travel in time and space. Neuron 2014; 81:728–39. [PubMed: 24559669]
17. Liddelow SA, Guttenplan KA, Clarke LE, Bennett FC, Bohlen CJ, Schirmer L, et al. Neurotoxic reactive astrocytes are induced by activated microglia. Nature 2017; 541:481–7. [PubMed: 28099414]
18. Mciver SR, Faideau M, Haydon PG. Neural-immune interactions in brain function and alcohol related disorders. New York: Springer Science+Business Media; 2012.
19. Hong JH, Chiang CS, Campbell IL, Sun JR, Withers HR, McBride WH. Induction of acute phase gene expression by brain irradiation. Int J Radiat Oncol Biol Phys 1995; 33:619–26. [PubMed: 7558951]
20. Yuan H, Gaber MW, Boyd K, Wilson CM, Kiani MF, Merchant TE. Effects of fractionated radiation on the brain vasculature in a murine model: blood-brain barrier permeability, astrocyte proliferation, and ultrastructural changes. Int J Radiat Oncol Biol Phys 2006; 66:860–6. [PubMed: 17011458]
21. Akiyama K, Tanaka R, Sato M, Takeda N. Cognitive dysfunction and histological findings in adult rats one year after whole brain irradiation. Neurol Med Chir (Tokyo) 2001; 41:590–8. [PubMed: 11803584]
22. Acharya MM, Baulch JE, Lusardi TA, Allen BD, Chmielewski NN, Baddour AA, et al. Adenosine kinase inhibition protects against cranial radiation-induced cognitive dysfunction. Front Mol Neurosci 2016; 9:42. [PubMed: 27375429]
23. Zhou H, Liu Z, Liu J, Wang J, Zhou D, Zhao Z, et al. Fractionated radiation-induced acute encephalopathy in a young rat model: cognitive dysfunction and histologic findings. AJNR Am J Neuroradiol 2011; 32:1795–800. [PubMed: 21920857]

24. Stevens B, Allen NJ, Vazquez LE, Howell GR, Christopherson KS, Nouri N, et al. The classical complement cascade mediates CNS synapse elimination. Cell 2007; 131:1164–78. [PubMed: 18083105]
25. Tenner AJ, Stevens B, Woodruff TM. New tricks for an ancient system: Physiological and pathological roles of complement in the CNS. Mol Immunol 2018; 102:3–13. [PubMed: 29958698]
26. Alexander JJ, Anderson AJ, Barnum SR, Stevens B, Tenner AJ. The complement cascade: Yin-yang in neuroinflammation–neuroprotection and -degeneration. J Neurochem 2008; 107:1169–87. [PubMed: 18786171]
27. Veerhuis R, Nielsen HM, Tenner AJ. Complement in the brain. Mol Immunol 2011; 48: 1592–603. [PubMed: 21546088]
28. Hong S, Beja-Glasser VF, Nfonoyim BM, Frouin A, Li S, Ramakrishnan S, et al. Complement and microglia mediate early synapse loss in Alzheimer mouse models. Science 2016; 352:712–16. [PubMed: 27033548]
29. Shi Q, Colodner KJ, Matousek SB, Merry K, Hong S, Kenison JE, et al. Complement C3-deficient mice fail to display age-related hippocampal decline. J Neurosci 2015; 35:13029–42. [PubMed: 26400934]
30. Vasek MJ, Garber C, Dorsey D, Durrant DM, Bollman B, Soung A, et al. A complement-microglial axis drives synapse loss during virus-induced memory impairment. Nature 2016; 534:538–43. [PubMed: 27337340]
31. Fonseca MI, Zhou J, Botto M, Tenner AJ. Absence of C1q leads to less neuropathology in transgenic mouse models of Alzheimer's disease. J Neurosci 2004; 24:6457–65. [PubMed: 15269255]
32. Klos A, Tenner AJ, Johswich KO, Ager RR, Reis ES, Kohl J. The role of the anaphylatoxins in health and disease. Mol Immunol 2009; 46:2753–66. [PubMed: 19477527]
33. Yao J, Harvath L, Gilbert DL, Colton CA. Chemotaxis by a CNS macrophage, the microglia. J Neurosci Res 1990; 27:36–42. [PubMed: 2254955]
34. Kalm M, Andreasson U, Bjork-Eriksson T, Zetterberg H, Pekny M, Blennow K, et al. C3 deficiency ameliorates the negative effects of irradiation of the young brain on hippocampal development and learning. Oncotarget 2016; 7:19382–94. [PubMed: 27029069]
35. Acharya MM, Baulch JE, Lusardi T, Allen BD, Chmielewski NN, Baddour AAD, et al. Adenosine kinase inhibition protects against cranial radiation-induced cognitive dysfunction. Front Mol Neurosci 2016; 9:1–10. [PubMed: 26834556]
36. Acharya MM, Green KN, Allen BD, Najafi AR, Syage A, Minasyan H, et al. Elimination of microglia improves cognitive function following cranial irradiation. Sci Rep 2016; 6:31545. [PubMed: 27516055]
37. Jorge PG, Jaccard M, Petersson K, Gondre M, Duran MT, Desorgher L, et al. Dosimetric and preparation procedures for irradiating biological models with pulsed electron beam at ultra-high dose-rate. Radiother Oncol 2019; 139:34–9. [PubMed: 31174897]
38. Jaccard M, Petersson K, Buchillier T, Germond JF, Duran MT, Vozenin MC, et al. High dose-per-pulse electron beam dosimetry: Usability and dose-rate independence of EBT3 Gafchromic films. Med Phys 2017; 44:725–35. [PubMed: 28019660]
39. Petersson K, Jaccard M, Germond JF, Buchillier T, Bochud F, Bourhis J, et al. High dose-per-pulse electron beam dosimetry – A model to correct for the ion recombination in the Advanced Markus ionization chamber. Med Phys 2017; 44:1157–67. [PubMed: 28094853]
40. Ingram G, Loveless S, Howell OW, Hakobyan S, Dancey B, Harris CL, et al. Complement activation in multiple sclerosis plaques: an immunohistochemical analysis. Acta Neuropathol Commun 2014; 2:53. [PubMed: 24887075]
41. Aronica E, Boer K, van Vliet EA, Redeker S, Baayen JC, Spliet WG, et al. Complement activation in experimental and human temporal lobe epilepsy. Neurobiol Dis 2007; 26:497–511. [PubMed: 17412602]
42. Iram T, Trudler D, Kain D, Kanner S, Galron R, Vassar R, et al. Astrocytes from old Alzheimer's disease mice are impaired in Abeta uptake and in neuroprotection. Neurobiol Dis 2016; 96:84–94. [PubMed: 27544484]

43. Orre M, Kamphuis W, Osborn LM, Jansen AHP, Kooijman L, Bossers K, et al. Isolation of glia from Alzheimer's mice reveals inflammation and dysfunction. Neurobiol Aging 2014; 35:2746–60. [PubMed: 25002035]
44. Wu T, Dejanovic B, Gandham VD, Gogineni A, Edmonds R, Schauer S, et al. Complement C3 is activated in human AD brain and is required for neurodegeneration in mouse models of amyloidosis and tauopathy. Cell Rep 2019; 28:2111–23 e6. [PubMed: 31433986]
45. McBride WH. Cytokine cascades in late normal tissue radiation responses. Int J Radiat Oncol Biol Phys 1995; 33:233–4. [PubMed: 7642425]
46. Hajishengallis G, Lambris JD. Crosstalk pathways between Toll-like receptors and the complement system. Trends Immunol 2010; 31:154–63. [PubMed: 20153254]
47. Roh JS, Sohn DH. Damage-associated molecular patterns in inflammatory diseases. Immune Netw 2018; 18:e27. [PubMed: 30181915]
48. Pekny M, Pekna M. Astrocyte reactivity and reactive astrogliosis: costs and benefits. Physiol Rev 2014; 94:1077–98. [PubMed: 25287860]
49. Hinkle JJ, Olschowka JA, Love TM, Williams JP, O'Banion MK. Cranial irradiation mediated spine loss is sex-specific and complement receptor-3 dependent in male mice. Sci Rep 2019; 9:18899. [PubMed: 31827187]
50. Spitz DR, Buettner GR, Petronek MS, St-Aubin JJ, Flynn RT, Waldron TJ, et al. An integrated physico-chemical approach for explaining the differential impact of FLASH versus conventional dose-rate irradiation on cancer and normal tissue responses. Radiother Oncol 2019; 139:23–7. [PubMed: 31010709]

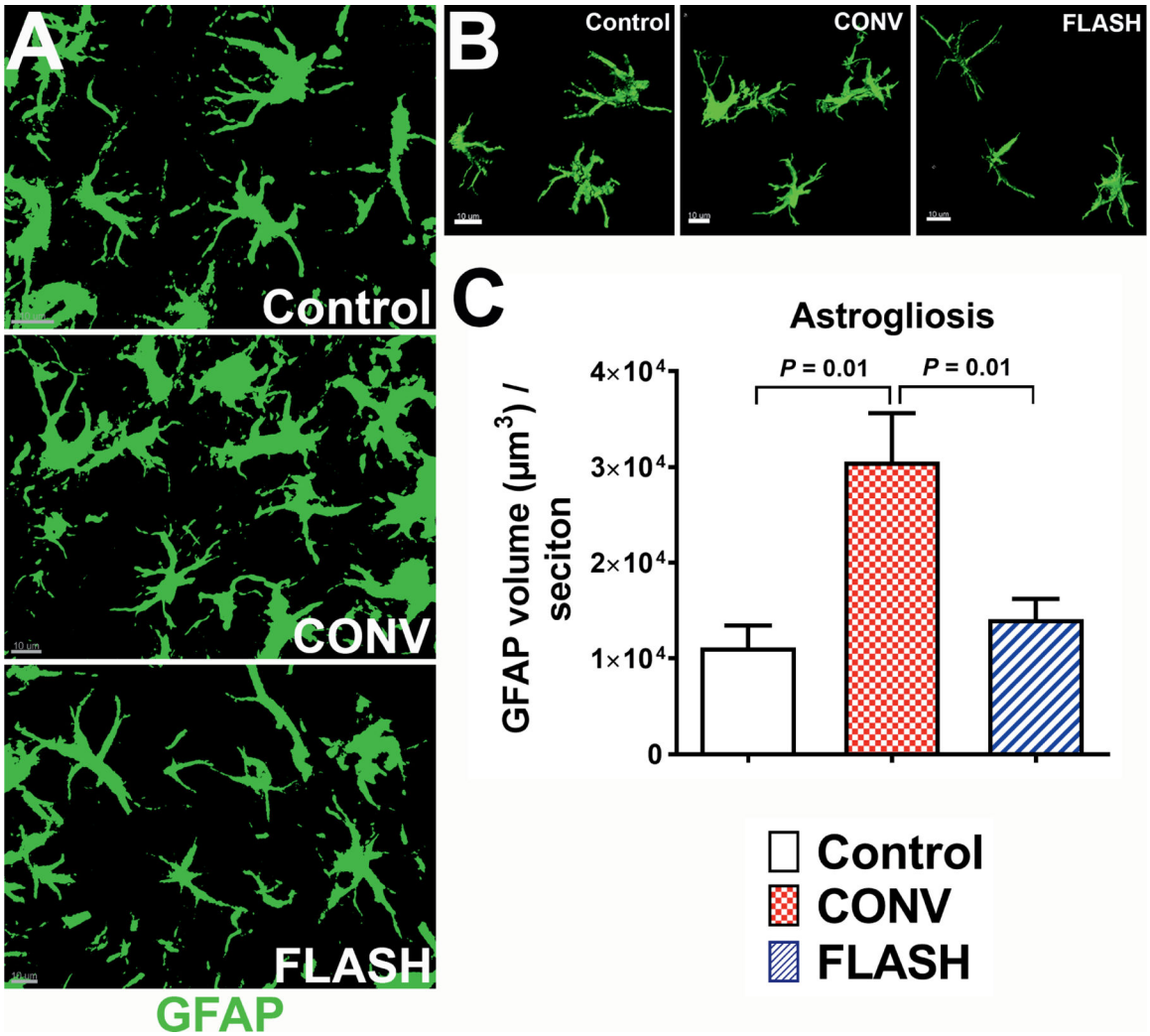

FIG. 1.

FLASH-RT did not induce astrocytic hypertrophy. Representative z stacks from laser scanning confocal microscopy (green, panel A) and volumetric analysis of 3D reconstruction for hippocampal astrocytes (green, GFAP, panel B) showed increased soma volume with thicker and longer stelae indicating astrocytic hypertrophy one month after 10 Gy CONV-RT. The astrocytic morphology in the FLASH-irradiated group was comparable to controls (panel C). Data are presented as mean ± SEM (n = 6 animals per group). *P* values are derived from non-parametric Kruskal-Wallis H test and Mann-Whitney's comparison between each group as indicated. Scale bar = 10 μm (panels A and B).

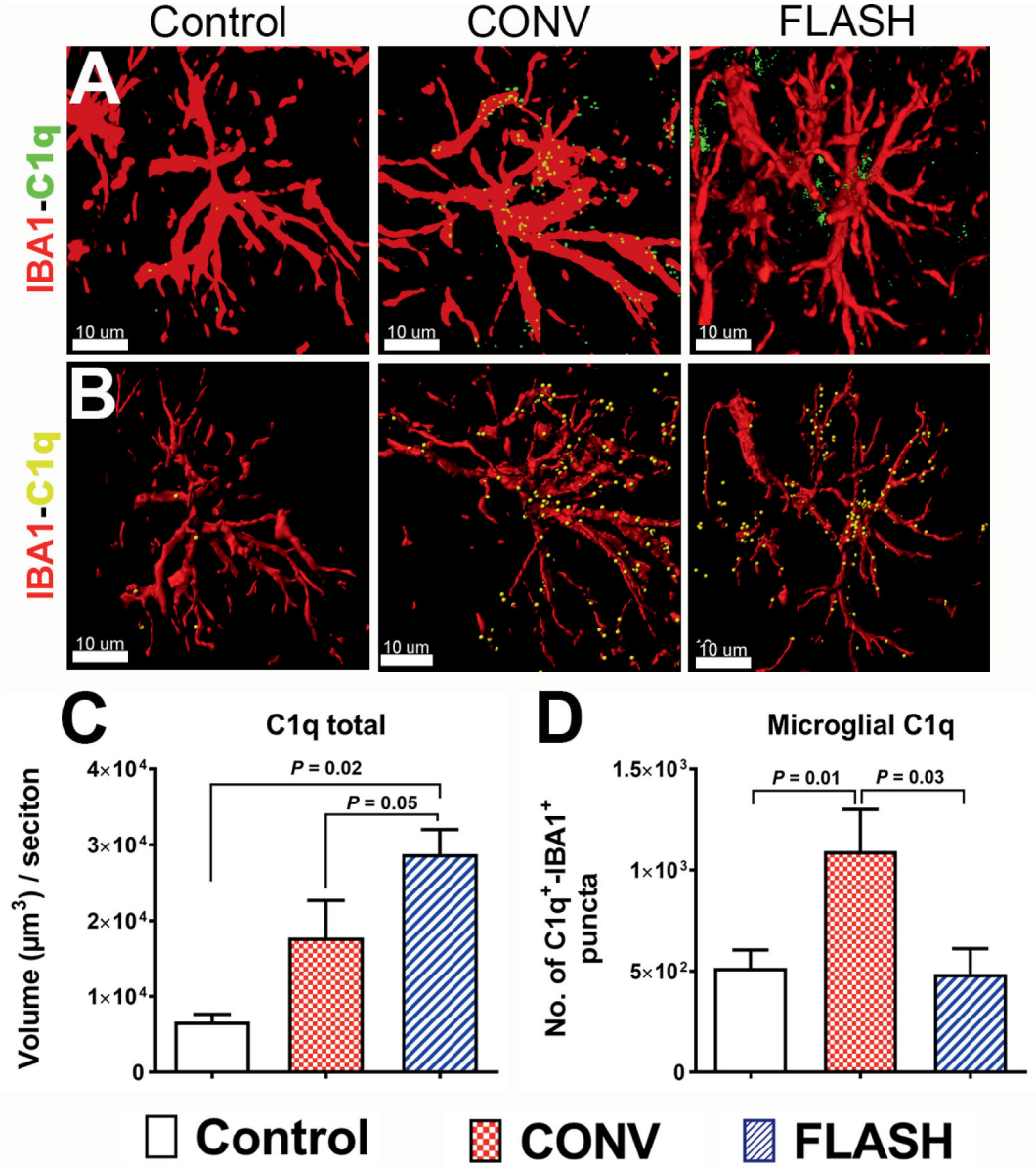

FIG. 2.

FLASH-RT of the brain did not elevate microglial expression of complement C1q. Confocal z stacks (red, IBA1; green, C1q, panel A) and 3D algorithm-based volumetric quantification of microglia (red, panel B) co-labeled with C1q (yellow spots, panel B) showed an increased total C1q expression (panel C) in the hippocampus after both irradiation modalities (10 Gy). One month after 10 Gy CONV-RT, there was significantly elevated microglial co-labeling of C1q in the hippocampus (panel D), whereas after FLASH-RT this was not observed. Data are presented as mean ± SEM (n = 4–6 animals per group). *P* values are derived from non-parametric Kruskal-Wallis H test and Mann-Whitney's comparison between each group as indicated. Scale bar = 10 μm (panels A and B).

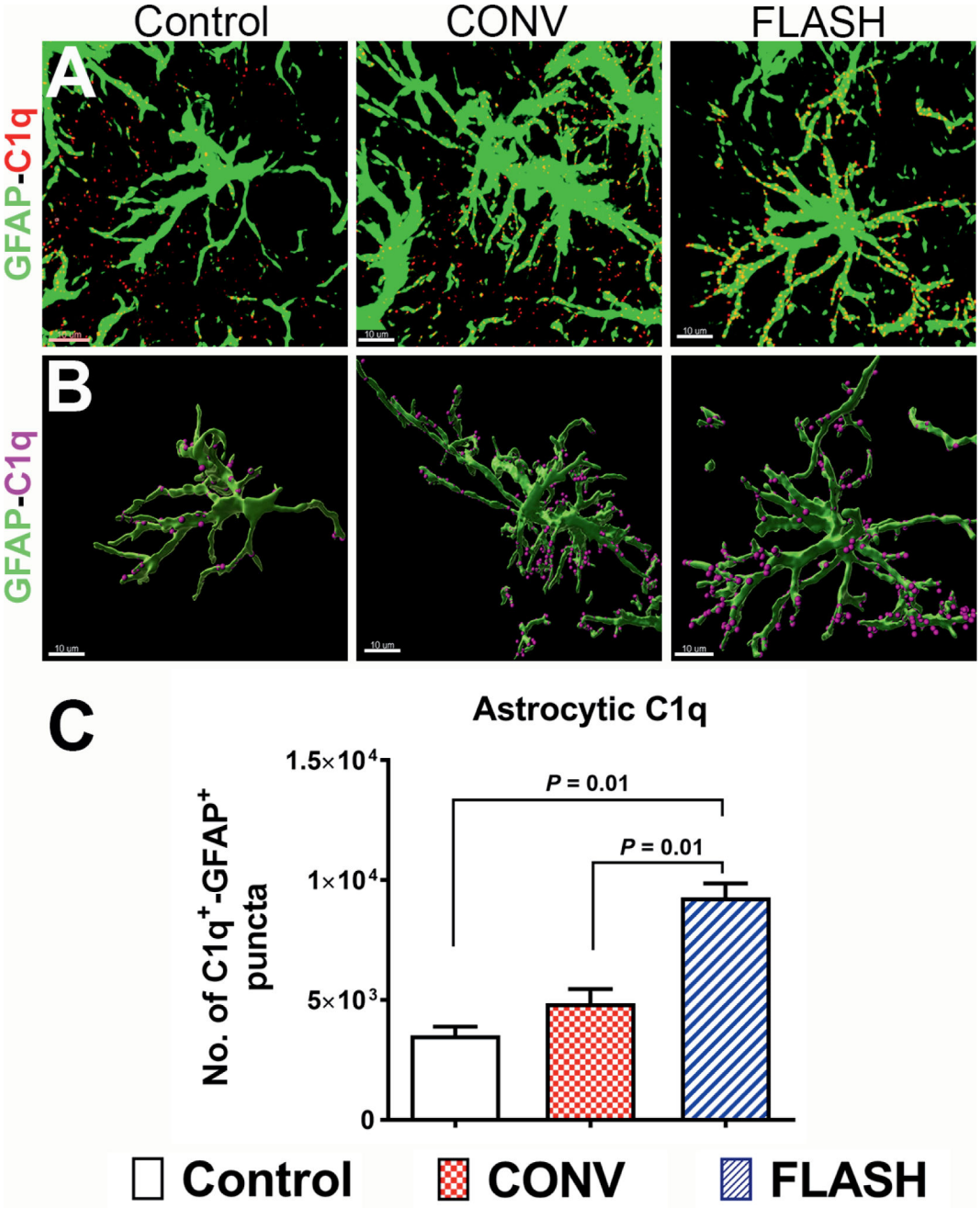

FIG. 3.

Elevated astrocytic expression of complement C1q in the irradiated brain. Volumetric quantification of confocal z stacks (green, GFAP; red, C1q, panel A) and 3D reconstruction of GFAP$^+$ astrocytes (green, panel B) co-labeled with C1q (magenta spots, panel B) showed a significantly elevated complement C1q one month after either 10 Gy CONV-RT or FLASH-RT (panel C). Data are presented as mean ± SEM (n = 4–6 animals per group). *P* values are derived from non-parametric Kruskal-Wallis H test and Mann-Whitney's comparison between each group as indicated. Scale bar = 10 μm (panels A and B).

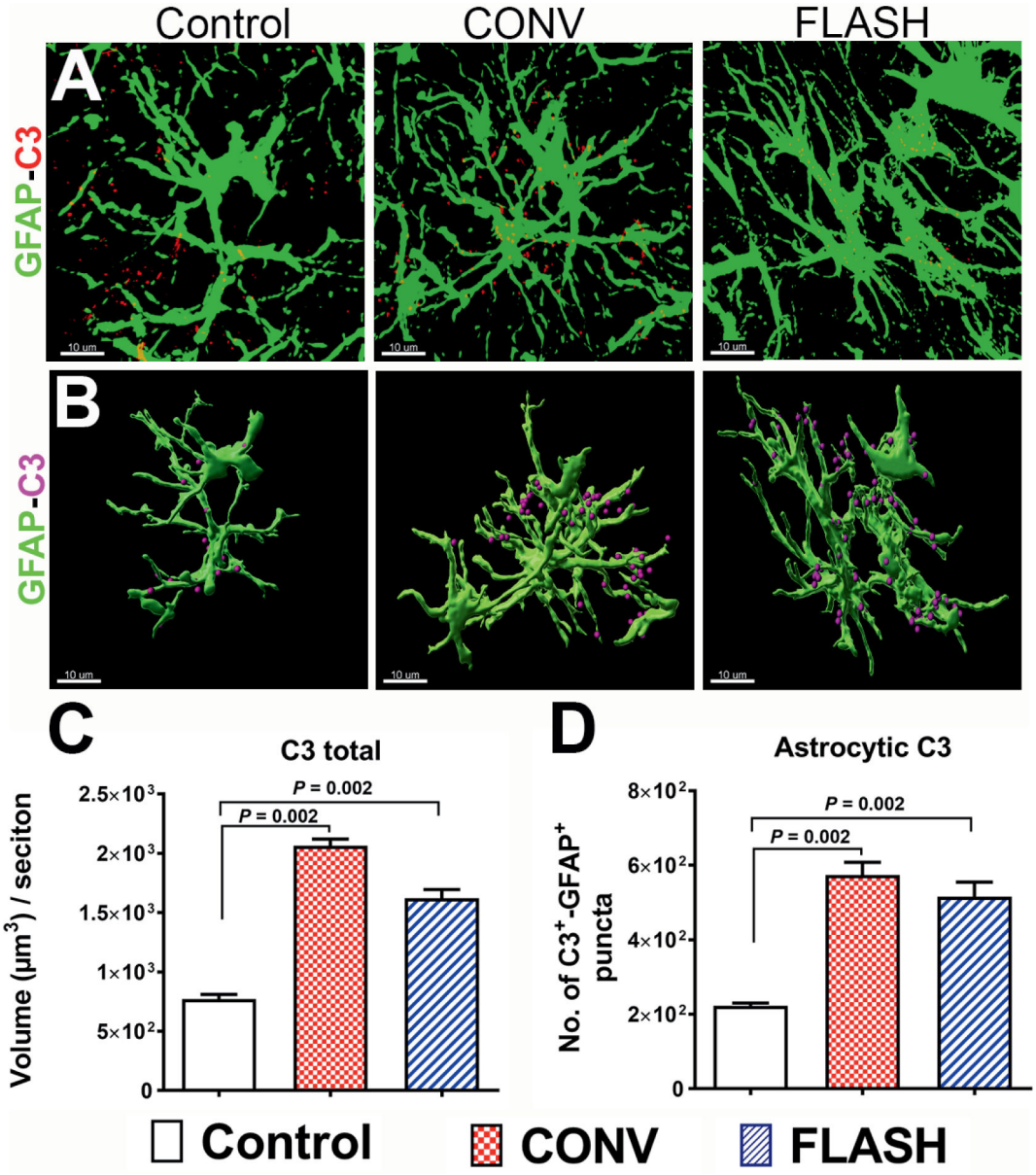

FIG. 4.

Cranial irradiation increased astrocytic co-labeling of complement C3 in the hippocampus. Representative z stacks from laser scanning confocal microscopy (green, GFAP; red, C3, panel A) and volumetric quantification of 3D rendered $GFAP^+$ astrocytes (green, panel B) showed a significantly elevated total C3 and GFAP co-labeling with C3 (magenta spots, panel B) one month after either 10 Gy CONV-RT or FLASH-RT (panel C). Data are presented as mean ± SEM (n = 6 animals per group). *P* values are derived from non-parametric Kruskal-Wallis H test and Mann-Whitney's comparison between each group as indicated. Scale bar = 10 µm (panel A and B).

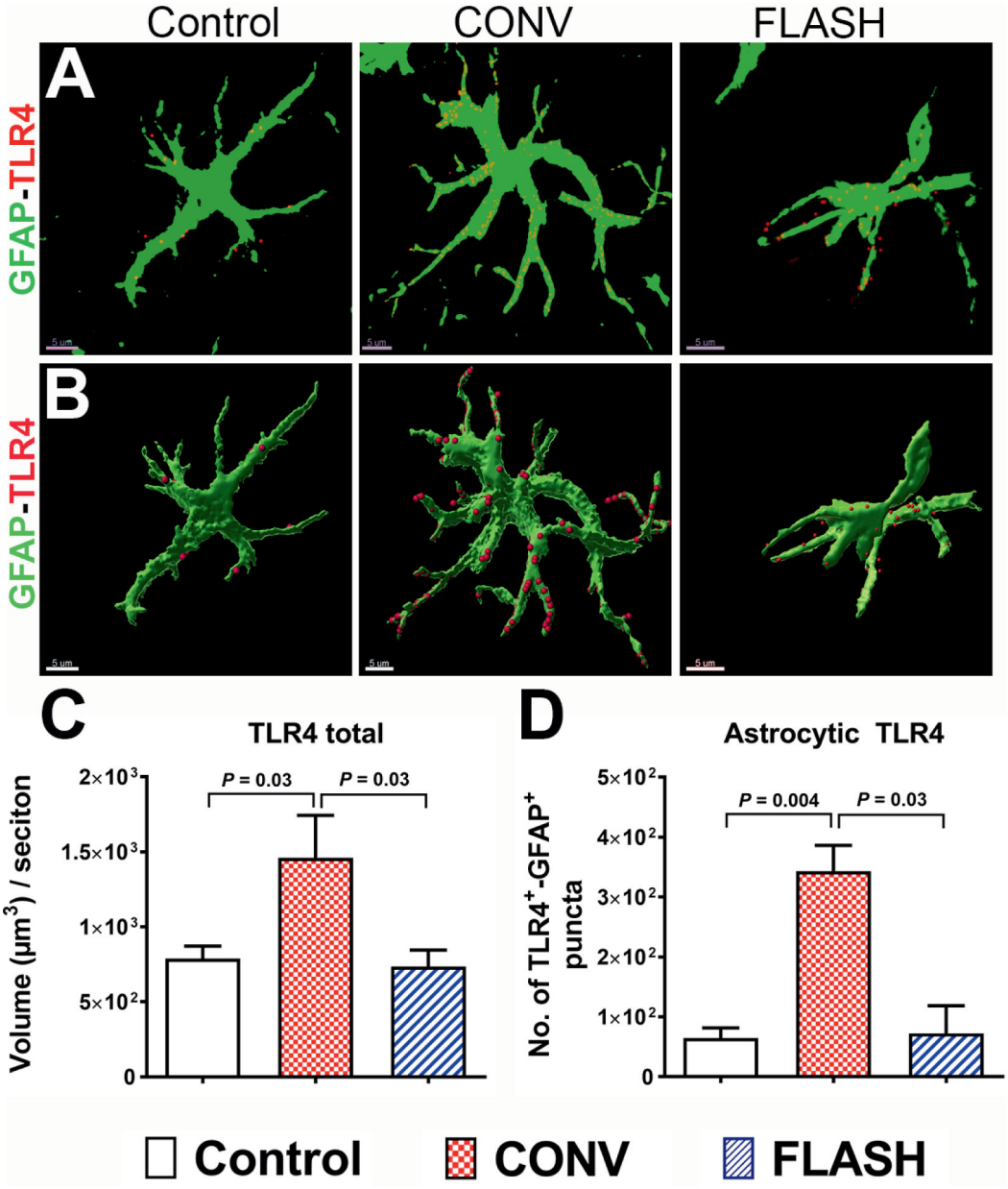

FIG. 5.

FLASH-RT did not elevate astrocytic expression of the danger receptor TLR4. Volumetric quantification of confocal z stacks (green, GFAP; red, TLR4, panel A) and 3D reconstruction of $GFAP^+$ surface (green, panel B) co-labeled with TLR4 (red, panel B) showed a significantly elevated total TLR4 and co-labeling with the danger-sensing receptor TLR4 one month after CONV-RT (panels C and D). Data are presented as Mean ± SEM (n = 5–6 animals per group). *P* values are derived from non-parametric Kruskal-Wallis H test and Mann-Whitney's comparison between each group as indicated. Scale bar = 5 μm (panels A and B).

TABLE 1:

Irradiation Parameters

Single doses WBRT		Beam parameters				
Mode	**Prescribed dose**	**Frequency (Hz)**	**SSD (mm)**	**Pulse width (μs)**	**No. of pulses**	**Treatment time (s)**
CONV	10 Gy	10	800	1.0	1,170–1,180	116.9–117.9
FLASH	10 Gy	100	369–370	1.8	1	$1.8 \cdot 10^{-6}$